Exchange Coupling Approach to the Radical Disposition of an Intermediate in *Escherichia coli* Ribonucleotide Reductase

Natarajan Ravi* and Emile L. Bominaar

Department of Chemistry, Carnegie Mellon University, Pittsburgh, Pennsylvania 15213

Received October 7, 1994[⊗]

Recent rapid freeze−quench EPR and Mössbauer studies have given evidence for the presence of an intermediate species, a spin-coupled trimer consisting of two high-spin ferric ions and a radical, in the cofactor assembly reaction of the R2 subunit in *Escherichia coli* ribonucleotide reductase (Ravi, N.; Bollinger, J. M.; Huynh, B. H.; Edmondson, D. E.; Stubbe, J. *J. Am. Chem. Soc.* **1994**, *116*, 8007). In the present study the radical disposition of this intermediate is investigated from the exchange-coupling perspective. A spin trimer with $S_1 = S_2 = {}^5/_2$ and $S_3 = {}^1/_2$ is analyzed in the framework of the Heisenberg−Dirac−Van Vleck formalism considering the most general case in which all the exchange-coupling constants are assumed to be unequal. The acceptable range, $0.66 < J_{13}/J_{23} < 1$, for the ratio of the exchange-coupling constants between the radical and the two iron sites strongly suggests that the radical ligand asymmetrically bridges the two iron atoms.

Introduction

Structural characterization of metal centers in enzymes plays a pivotal role in elucidating their mechanistic pathways. The study of exchange coupling may offer a useful alternative means of gaining information about reactive intermediates,[1,2] particularly when the crystal structure is inaccessible. Strong exchange couplings ($J \sim 80-250$ cm^{-1}, in $JS_1 \cdot S_2$ convention) are found in the diferric state of μ-oxo bridged binuclear iron centers in enzymes such as hemerythrin, purple acid phosphatase, Δ^9-desaturase, and ribonucleotide reductase.[3−6] By analogy, a strong exchange coupling can be surmised for the binuclear center containing protein rubrerythrin from the similarity of the spectroscopic properties with those of the proteins mentioned above.[7] Weak exchange couplings ($J \sim 40$ cm^{-1}) are observed in the diferric state of a number of μ-hydroxo-bridged model compounds.[8,9] The weak exchange coupling found in the diferric state of methane monooxygenase has been used to suggest that the bridging ligand is a substituted oxygen atom.[10] The suggestion is corroborated by a recent study of the crystal structure of this enzyme in which the bridging ligand is reported to be a μ-hydroxo species.[11] In fact, the presence of either a strong or a weak exchange coupling has almost become a diagnostic test to infer the nature of the bridging ligand in binuclear systems: an oxo bridge mediates strong exchange interaction whereas a non-oxo bridge, such as hydroxo or carboxylato, yields weak exchange. Furthermore, weak couplings have been reported in the fully reduced state of hemerythrin, purple acid phosphatase, and ribonucleotide reductase in which the metal ions are high-spin ferrous.[12−14]

Recently, rapid freeze−quench EPR and Mössbauer techniques have been successfully employed to gain more insight into the mechanism of the cofactor assembly of the R2 subunit in *Escherichia coli* ribonucleotide reductase (R2) by monitoring the rise−fall behavior of a kinetically competent reactive intermediate species designated as "X".[15,16] The isotropic EPR resonance at $g \approx 2.0$, the isomer shift, and the magnetic hyperfine constants of opposing sign deduced from the Mössbauer data unequivocally prove that, in this intermediate, the spins of two high-spin ferric ions are coupled to a third spin, presumably a radical species, to give a resultant system spin $S = {}^1/_2$. The analysis precludes that the intermediate is a spin-coupled Fe(III)−Fe(IV) dimer.[16a] A similar study, carried out for the enzyme methane monooxygenase from *Methylosinus trichosporium* OB3b showed that the catalytic process involves an intermediate species, designated as "Q", containing two antiferromagnetically coupled Fe(IV) ions, resulting in a diamagnetic ground state. This intermediate, in which the two iron sites are indistinguishable, has been proposed to contain

[⊗] Abstract published in *Advance ACS Abstracts,* February 1, 1995.

(1) Kahn, O. *Molecular Magnetism*; VCH Publishers: New York, 1993.
(2) Bencini, A.; Gatteschi, D. *Electron Paramagnetic Resonance of Exchange Coupled Systems*; Springer-Verlag: Berlin, Heidelberg, 1990.
(3) (a) Moss, T. H.; Moleski, C.; York, J. L. *Biochemistry* **1971**, *10*, 840−842. (b) Okamura, M. Y.; Klotz, I. M.; Johnson, C. E.; Winter, M. R. C.; Williams, R. J. P. *Biochemistry* **1969**, *8*, 1951−1958.
(4) Lauffer, R. B.; Antanaitis, B. C.; Aisen, P.; Que, L. *J. Biol. Chem.* **1983**, *258*, 14212−14218.
(5) Fox, B. G.; Shanklin, J.; Somerville, C.; Münck, E. *Proc. Natl. Acad. Sci. U.S.A.* **1991**, *90*, 2486−2490.
(6) (a) Petersson, L.; Gräslund, A.; Ehrenberg, A.; Sjöberg, B.-M.; Reichard, P. *J. Biol. Chem.* **1980**, *255*, 6706−6712. (b) Hirsh, D. J.; Beck, W. F.; Lynch, J. B.; Que, L.; Brudwig, G. W. *J. Am. Chem. Soc.* **1992**, *114*, 7475−7481. (c) Sjöberg, B.-M.; Loehr, T. M.; Sanders-Loehr, J. *Biochemistry* **1982**, *21*, 96−102.
(7) (a) Ravi, N.; Prickril, B. C.; Kurtz, D. M.; Huynh, B. H. *Biochemistry* **1993**, *32*, 8487−8491. (b) Dave, B. C.; Czernuszewicz, R. S.; Prickril, B. C.; Kurtz, D. M. *Biochemistry* **1994**, *33*, 3572−3576.
(8) Turowski, P. N.; Armstrong, W. H.; Liu, S.; Brown, S. N.; Lippard, S. J. *Inorg. Chem.* **1994**, *33*, 636−645.
(9) Wu, F.-J.; Kurtz, D. M.; Hagen, K. S.; Nyman, P. D.; Debrunner, P. G.; Vankai, V.A. *Inorg. Chem.* **1990**, *29*, 5174−5183.
(10) Fox, B. G.; Hendrich, M. P.; Surerus, K. K.; Anderson, K. K.; Froland, W. A.; Lipscomb, J. D.; Münck, E. *J. Am. Chem. Soc.* **1993**, *115*, 3688−3701.
(11) Rosenzweig, A. C.; Frederick, C. A.; Lippard, S. J.; Nordlund, P. *Nature* **1993**, *366*, 537−543.
(12) Reem, R. C.; Solomon, E. I. *J. Am. Chem. Soc.* **1987**, *109*, 1216−1226.
(13) Que, L.; True, A. E. *Prog. Inorg. Chem.: Bioinorg Chem.* **1990**, *38*, 97−200.
(14) Atta, M.; Dalton, H.; Fontecave, M.; Fries, P. H.; Jacquot, J. F.; Latour, J. M.; Wilkins, P. *J. Inorg. Biochem.* **1993**, *51*, 455.
(15) (a) Bollinger, J. M., Jr.; Stubbe, J.; Huynh, B. H.; Edmondson, D. E. *J. Am. Chem. Soc.* **1991**, *113*, 6289−6291. (b) Bollinger, J. M., Jr. Ph.D. Thesis, M.I.T., Cambridge, MA, 1993.
(16) (a) Ravi, N.; Bollinger, J. M., Jr.; Huynh, B. H.; Edmondson, D. E.; Stubbe, J. *J. Am. Chem. Soc.* **1994**, *116*, 8007−8014. (b) Bollinger, J. M., Jr.; Tong, W. H.; Ravi, N.; Huynh, B. H.; Edmondson, D. E.; Stubbe, J. *J. Am. Chem. Soc.* **1994**, *116*, 8015−8023. (c) Bollinger, J. M., Jr .; Tong, W. H.; Ravi, N.; Huynh, B. H.; Edmondson, D. E.; Stubbe, J. *J. Am. Chem. Soc.* **1994**, *116*, 8024−8032.

0020-1669/95/1334-1040$09.00/0

either a single oxygen atom bridging the two iron centers or two equivalent oxygen atoms in one of the possible configurations for a diferryl unit.[17] Another intermediate of the same enzyme from *Methylococcus capsulatus* (Bath), designated as "L", presumably the precursor for the formation of Q, is suggested to be a diamagnetic (μ-peroxo)diferric species in an $\eta^1-\eta^1$ or $\eta^2-\eta^2$ bridging mode.[18] While there exists a variety of structural motifs for these intermediates, only two possible structures have been envisaged for the intermediate "X" of R2 based on the crystallographic data of the diferric and diferrous states of the enzyme:[19,20] one considers the radical to be a terminal ligand, probably OH•, for one of the iron sites, while the other suggests the radical as a bridging ligand.[16a] Despite a high degree of sequence homology and structural similarity of the active sites in the two enzymes, the reaction kinetics appear to proceed via different paths and intermediates.

As noted above, the Mössbauer data of the reactive intermediate of R2 reveal two magnetically distinct iron sites. In the interpretation of the magnetic hyperfine parameters (A_i values) of the iron sites,[16a] the general form of a spin $S = {}^1/_2$ state in the three-spin system with $S_1 = {}^5/_2$, $S_2 = {}^5/_2$, $S_3 = {}^1/_2$ was considered, $(1 - \alpha^2)^{1/2}|S_{23} = 2\rangle - \alpha|S_{23} = 3\rangle$, which is a linear combination of two basis states (see below). The magnetic hyperfine coupling constants, A_i, for the iron sites of the composite system in the general $S = {}^1/_2$ state were then expressed in terms of the intrinsic high-spin ferric hyperfine parameters, a_i, and the mixing coefficient, α. If an a_i value of -22 T is adopted,[21] typical for high-spin ferric iron in N/O coordination, the theoretical expressions for A_i were found to closely match the values of the experimental hyperfine parameters of the *two* iron sites of the trinuclear unit for a *single* value of the mixing coefficient α (+0.21). In the present work, the $S = {}^1/_2$ state, deduced from the spectroscopic data, is analyzed in the framework of the Heisenberg–Dirac–Van Vleck (HDVV) formalism. The allowed ranges of the values for the iron–iron and iron–radical exchange-coupling constants (ecc), which are compatible with the spin ground state, are derived. Finally, conclusions are drawn from the ecc obtained as to where the radical in the intermediate resides.

Description of the Model

We adopt in our analysis the usual HDVV Hamiltonian

$$H = J_{12}S_1{\cdot}S_2 + J_{23}S_2{\cdot}S_3 + J_{13}S_1{\cdot}S_3 \qquad (1)$$

where S_1, S_2, and S_3 denote the spin operators of the two iron sites and the radical, respectively, and J_{ij} the ecc between the sites i and j. As basis set for the spin space, we have chosen the states

$$|S_{23},S\rangle = |(S_2 = {}^5/_2, S_3 = {}^1/_2)S_{23}, S_1 = {}^5/_2; S\rangle \qquad (2)$$

These states are constructed by coupling S_2 and S_3 to resultant subspin S_{23} and then coupling S_{23} with S_1 to obtain system spin S. For $S = {}^1/_2$ to ${}^9/_2$, the subspin quantum number S_{23} is equal to 2 or 3; for $S = {}^{11}/_2$, only $S_{23} = 3$ is possible. The matrix elements of eq 1 are calculated by straightforward application of spin-coupling techniques.[2] The resulting submatrix for $S = {}^1/_2$ is

$$\begin{matrix} \langle 2,{}^1/_2| \\ \langle 3,{}^1/_2| \end{matrix} \begin{bmatrix} -{}^7/_4J_{23} + {}^7/_6J_{13} - {}^{49}/_6J_{12} & \frac{\sqrt{35}}{12}(J_{13} - J_{12}) \\ \frac{\sqrt{35}}{12}(J_{13} - J_{12}) & {}^5/_4J_{23} - {}^5/_3J_{13} - {}^{25}/_3J_{12} \end{bmatrix} \qquad (3)$$

The eigenstates of the matrix eq 3 are of the form

$$|{}^1/_2\rangle = \sqrt{(1 - \alpha^2)}|2,{}^1/_2\rangle - \alpha|3,{}^1/_2\rangle \qquad (4)$$

where α is a mixing coefficient.

The magnetic hyperfine coupling constant of the ith site, A_i, is related to the intrinsic coupling constant, a_i, by

$$A_i = 2a_i\langle {}^1/_2;+|S_{iz}|{}^1/_2;+\rangle \qquad (5)$$

where S_{iz} is the z-component of the spin operator of site i (i = 1, 2, 3) and + denotes the magnetic quantum number $M_S = {}^1/_2$ of the total spin. By using eq 4, the expectation value in eq 5 can be expressed in terms of the mixing coefficient α,[16a]

$$\langle {}^1/_2;+|S_{1z}|{}^1/_2;+\rangle = {}^7/_6 - 2\alpha^2$$

$$\langle {}^1/_2;+|S_{2z}|{}^1/_2;+\rangle = {}^1/_9[17\alpha^2 + \sqrt{35}\alpha\sqrt{1 - \alpha^2} - 7] \qquad (6)$$

$$\langle {}^1/_2;+|S_{3z}|{}^1/_2;+\rangle = {}^1/_9[\alpha^2 - \sqrt{35}\alpha\sqrt{1 - \alpha^2} + 1]$$

At this point, it is convenient to introduce the ratio r of the matrix elements occurring in eq 3, defined as

$$r = \frac{\langle 2,{}^1/_2|H|3,{}^1/_2\rangle + \langle 3,{}^1/_2|H|2,{}^1/_2\rangle}{\langle 2,{}^1/_2|H|2,{}^1/_2\rangle - \langle 3,{}^1/_2|H|3,{}^1/_2\rangle} = \frac{\sqrt{35}(J_{13} - J_{12})}{-18J_{23} + 17J_{13} + J_{12}} \qquad (7)$$

The mixing coefficient α and the ratio r are related by the expression

$$r = \pm\sqrt{\frac{1}{(2\alpha^2 - 1)^2} - 1} \qquad (8)$$

which is derived by calculating the eigenvectors of matrix eq 3 for a given ratio r. Equation 7 can be rewritten as

$$-18r + (17r - \sqrt{35})\frac{J_{13}}{J_{23}} + (r + \sqrt{35})\frac{J_{12}}{J_{23}} = 0 \qquad (9)$$

Hence, for a given value of $|\alpha|$, the solutions for the ecc are located on two lines in the $(J_{13}/J_{23},J_{12}/J_{23})$ plane which are obtained from eq 9 by substituting the r values of opposite sign given in eq 8. The solutions run through the point (1,1) where the three ecc values are equal; this solution yields a degenerate ground state with spin $S = {}^1/_2$ in the case of antiferromagnetic coupling.

In order to avoid redundancy in the solutions and without loss of generality, we adopt the convention

$$J_{23} \geq J_{13} \qquad (10)$$

(17) Lee, S.-K.; Fox, B. G.; Froland, W. A.; Lipscomb, J. D.; Münck, E. *J. Am. Chem. Soc.* **1993**, *115*, 6450–6451.
(18) Liu, K. E.; Wang, D.; Huynh, B. H.; Edmondson, D. E.; Salifoglou, A.; Lippard, S. J. *J. Am. Chem. Soc.* **1994**, *116*, 7465–7466.
(19) Nordlund, P.; Sjöberg, B.-M.; Eklund, H. *Nature* **1990**, *345*, 593–598; Nordlund, P.; Eklund, H. *J. Mol. Biol.* **1993**, *232*, 123–164.
(20) Aberg, A. Ph.D. Thesis, Stockholm University, 1993, as quoted in ref 16a (ref 74).
(21) Energy units are converted to magnetic field units upon division by $g_N\beta_N$, where g_N is the ground-state g-factor of the ^{57}Fe nucleus and β_N the nuclear Bohr magneton.

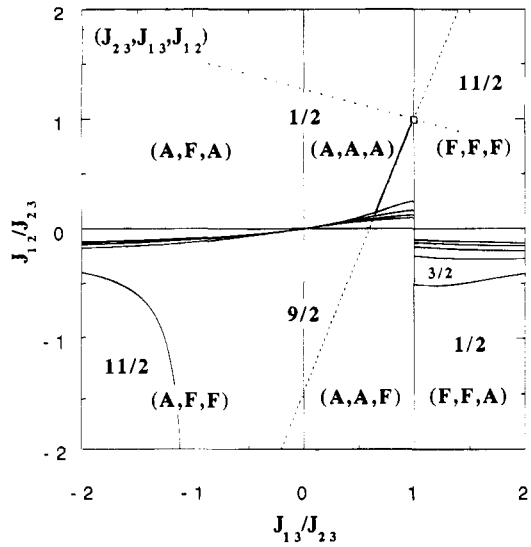

Figure 1. Spin-phase diagram for the Hamiltonian eq 1. The horizontal line defined by $J_{12}/J_{23} = 0$ and the vertical lines by $J_{13}/J_{23} = 0$ and 1 indicate domains with different combinations of ecc, i.e. ($J_{23} > 0$, $J_{13} < 0$, $J_{12} > 0$) ≡ (A, F, A) etc., of ferromagnetic ($J_{ij} < 0$) and antiferromagnetic ($J_{ij} > 0$) signs. Boundaries of domains with ground state spin $S = {}^1/_2, \ldots, {}^{11}/_2$ are indicated by the curves and the vertical line defined by $J_{13}/J_{23} = 1$. Line (- - -) depicts solution for $\alpha = -0.21$, and line (•••) that for $\alpha = +0.21$. Solutions for $\alpha = +0.21$ which coincide with the ground state of the Hamiltonian are highlighted (—).

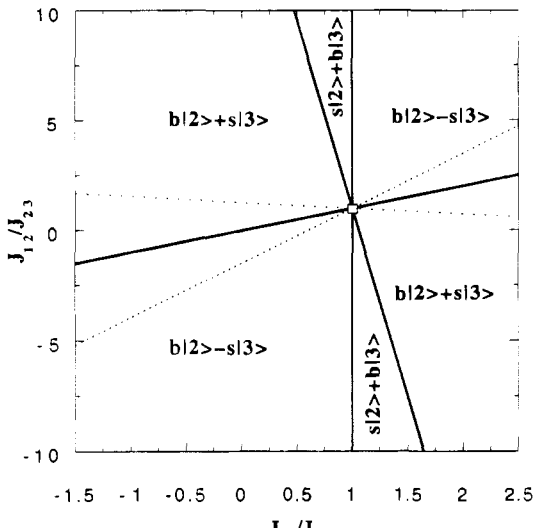

Figure 2. Lowest $S = {}^1/_2$ eigenstate of Hamiltonian eq 1 as a function of ratios J_{13}/J_{23} and J_{12}/J_{23}. **b** (>0) and **s** (>0) stand for coefficients of big and small magnitudes, respectively. The domains of indicated function type are marked by the three boldface lines running through point (1,1): $J_{13}/J_{23} = 1$, $J_{13}/J_{23} - J_{12}/J_{23} = 0$, $-18 + 17\,J_{13}/J_{23} + J_{12}/J_{23} = 0$. Line (- - -) depicts the solution for $\alpha = -0.21$, and line (•••) that for $\alpha = +0.21$.

(In the case of the opposite sign, the inequality can be met by relabeling 1, 2 into 2, 1). The possible combinations, satisfying eq 10, of ferromagnetic ($J < 0$, F) and antiferromagnetic ($J > 0$, A) exchange couplings are indicated in the (J_{13}/J_{23},J_{12}/J_{23}) plane given in Figure 1. Accordingly, the relative signs and magnitudes of the mixing coefficients in the lowest $S = {}^1/_2$ state are presented in Figure 2. The figure can be used to select the solution of required α-sign. Figure 1 displays furthermore the ground state spin of the HDVV Hamiltonian given in eq 1 as a function of the ratios J_{13}/J_{23} and J_{12}/J_{23}. This "spin-phase" diagram is constructed by comparison of the lowest energy eigenvalue obtained from eq 3 for $S = {}^1/_2$ and those

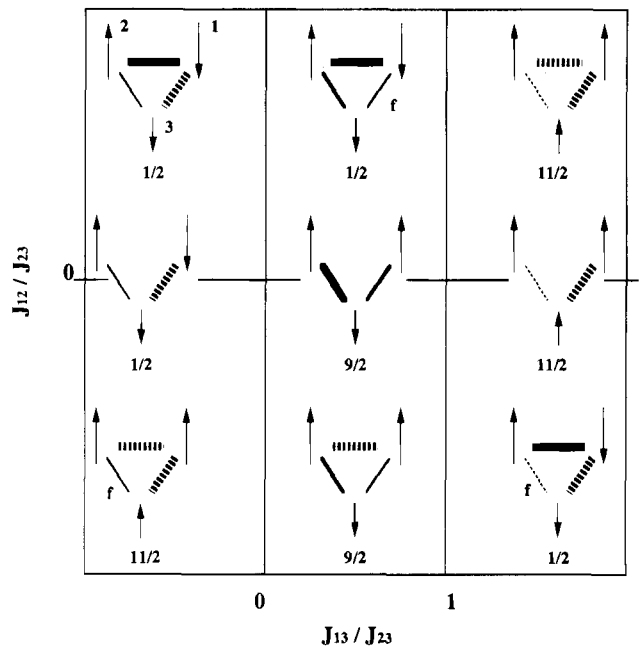

Figure 3. Schematic representation of spin states in the domains of spin-phase diagram given in Figure 1. Iron and radical spins are indicated by large and small arrows, respectively. Broken lines represent ferromagnetic couplings, and solid lines, antiferromagnetic couplings. Stronger couplings are depicted in boldface. Couplings labeled by f are "frustrated".

calculated from the secular problems in the states of higher spin. Schematic representations of the spin ground states, as obtained in the different domains of the spin-phase diagram, can be found in Figure 3.

Results and Discussion

The spin-Hamiltonian parameters obtained from the Mössbauer analysis of the intermediate in R2 are $A_{eff} = -52.5$ T, quadrupole splitting (ΔE_Q) = −1.0 mm s^{-1}, isomer shift (δ) = 0.55 mm s^{-1} for site 1 and $A_{eff} = +24.0$ T, $\Delta E_Q = -1.0$ mm s^{-1}, $\delta = 0.36$ mm s^{-1} for site 2. As mentioned in the Introduction, the three-spin coupling model reproduces both the magnitudes and the signs of the magnetic hyperfine parameters, A_i, for $a_i = -22$ T ($i = 1, 2$) and $\alpha = +0.21$.[16a] Substituting the latter value in eq 8 yields $r = \pm 0.45$. The values impose linear relationships between the ecc which are given in eq 9. These solutions, depicted by the two lines in Figures 1 and 2, have positive and negative slopes, of which the line with the negative slope is ignored as it corresponds to an $S = {}^1/_2$ state that has a mixing coefficient α of negative sign. The allowed solutions are located at the intersection of the line with the positive slope and the domain for ground state spin $S = {}^1/_2$ of the spin-phase diagram shown in Figure 1. The procedure leaves only the points on a finite line segment, indicated in Figure 1, as possible solutions, and it is seen that the three ecc values are antiferromagnetic ($J_{ij} > 0$). Figure 1 shows that the ratios of the two iron−radical coupling constants lie close to unity: $0.66 < J_{13}/J_{23} < 1$. For $J_{13}/J_{23} = 1$ the iron sites are magnetically equivalent, and this point is therefore excluded as possible solution. The exchange coupling between a terminal radical ligand and its coordinating iron site is expected, from orbital overlap considerations, to be at least one order of magnitude larger than the coupling between a radical and a noncoordinating iron site.[1] The allowed range of J_{13}/J_{23} ratios thus suggests that one of the proposed structures, viz. the one with the radical in a terminal position, can be ruled out. Further-

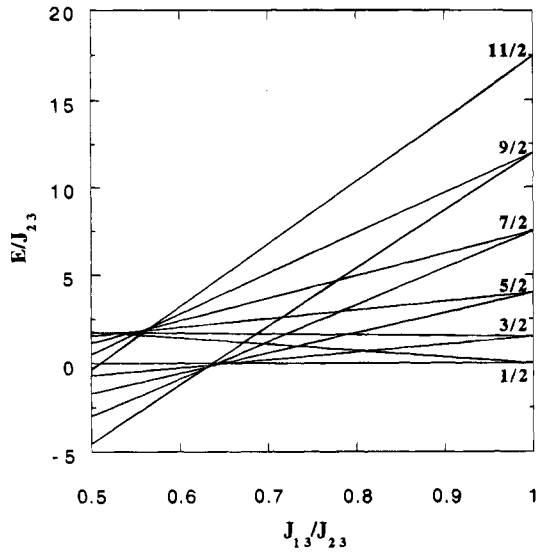

Figure 4. Relative ground and excited state energies of Hamiltonian eq 1 along the line in the (J_{13}/J_{23}, J_{12}/J_{23}) plane (Figure 1) containing the allowed solutions for the ecc in the intermediate of R2.

more, the ratio of the iron−iron coupling (J_{12}) and the largest iron−radical coupling (J_{23}) is confined to the range $0.15 < J_{12}/J_{23} < 1$.

The analysis presented above considers only the ratios of the exchange couplings. Predicted values for the relative energies of the ground and the excited states are presented in Figure 4. The first excited state with spin $S > {}^1/_2$ is a quartet separated from the ground state by an energy gap of less than ${}^3/_2J_{23}$. Although the magnitudes of the ecc have not been determined, Mössbauer data recorded in applied field (8 T) indicate that the energy gap should be larger than 8 cm^{-1}.[16a,22] In addition, a temperature dependent EPR study of the system shows an $S = {}^1/_2$ resonance, which persists up to 70 K,[15b] and gives no evidence of any thermal excited-state population, which is indicative of moderate or strong iron−radical coupling. Hence, the iron−radical linkages need to provide efficient exchange pathways in order to produce couplings of sufficient strength. The relative and absolute magnitudes of the ecc thus indicate that the radical asymmetrically bridges the two iron sites.

The intrinsic a values of high-spin ferric ions in N/O coordination range from −20 to −22 T depending on coordination number and covalency. A fit of the experimental magnetic hyperfine constants in the intermediate of R2 using a single, site-independent intrinsic a value, which is confined to the range mentioned, yields the optimal values $a = -22$ T and $\alpha = +0.21$ (eqs 5 and 6). The resulting A_1 value ($A_1 = -48$ T, $A_2 = +24$ T) differs slightly from the experimental number, $A_1 = -52$ T. An exact fit is possible if the intrinsic a_i values of the two sites are taken as independent adjustable parameters. Such a procedure leads to a range of solutions, comprising (i) the symmetric case $J_{13} = J_{23}$ for which the magnetic inequivalence of the iron sites is merely due to the difference in the intrinsic a_i values and (ii) the asymmetric case $J_{13} \neq J_{23}$ where the site inequivalence arises from both unequal coupling constants and differences in the a_i values. After imposition of the condition $(a_1 + a_2)/2 = -22$ T, the procedure yields a unique set of optimal values, $a_1 = -24$ T, $a_2 = -20$ T, and $\alpha = +0.19$, which are close to the numbers obtained from the procedure using equal a_i values. In other words, the optimal α value is almost independent of the fit procedure, provided the intrinsic a_i values lie near the acceptable range.

As the present work is related to the exchange interactions in a three-spin system, a brief comparison with other spin-trimers merits attention. Extensive studies, experimental as well as theoretical, have been performed on $[3Fe-4S]^{+,0}$ clusters.[23−25] The oxidized species of *Desulfovibrio gigas* ferredoxin (Fd II) contains three high-spin ferric ions coupled to a resultant spin $S = {}^1/_2$. The similarity of the iron−sulfur bridges gives rise to ecc ratios close to unity; the couplings recently reported in an NMR study of Fd II differ by only 2%.[26] The experimental data for the magnitude of the ecc in the cluster as obtained by different spectroscopic methods, viz. EPR, saturation magnetization, and NMR, are, however, ambiguous and amount to $J_{ij} \approx 40$, >200, and 300 cm^{-1}, respectively.[26−28] The values for the ecc in the intermediate of R2 are expected to be more dispersed than the couplings in the iron−sulfur cluster, due to the inequivalence of the iron and radical sites. As can be seen from Figure 1, the iron−radical couplings are stronger than the iron−iron couplings throughout the solution range. The relative strengths of the couplings may be related to the direct and indirect character of the exchange interactions in the iron−radical and iron−iron pathways, respectively. The solutions for the ecc show furthermore a slight disparity in the two iron−radical couplings, indicating that the bridging radical species is asymmetrically linked to the two iron sites.[29] It has been postulated from the line broadening observed in ^{17}O EPR experiments that the radical in the intermediate is an oxyl ($^{\bullet}O^{-}$) species.[16a] The present study gives strong evidence that this oxyl radical species is asymmetrically bridging the two iron sites of the reactive intermediate in R2.

Acknowledgment. The authors wish to acknowledge Dr. B. H. Huynh and Dr. E. Münck for encouragement, fruitful discussions, and helpful suggestions to improve the manuscript. This study is supported by the National Institutes of Health Grant GM22701 to Dr. E. Münck.

IC9411561

(22) In an applied magnetic field of 8 T, the Zeeman interaction lowers the energy of the $M_S = -{}^3/_2$ level of an excited spin $S = {}^3/_2$ state by $\Delta E = g\beta H_{app} \approx 8$ cm^{-1} relative to the $M_S = -{}^1/_2$ level of the ground state. Since no thermal occupation of the $S = {}^3/_2$ level is observed in the Mössbauer spectra, it is obvious that the spin quartet should lie more than 8 cm^{-1} above the ground state in the absence of a magnetic field. As the energy gap between the $S = {}^1/_2$ and $S = {}^3/_2$ states without field is less than ${}^3/_2J_{23}$ (see Figure 4), it can be concluded that J_{23} is larger than 6 cm^{-1}. A more accurate estimate of the ecc may be obtained from high-field, high-temperature Mössbauer spectra.

(23) Griffith, J. S. *Struct. Bonding* **1972**, *10*, 87−126.
(24) Kent, T. A.; Huynh, B. H.; Münck, E. *Proc. Natl. Acad. Sci. U.S.A.* **1980**, *77*, 6574−6576.
(25) Borshch, S. A.; Bominaar, E. L.; Blondin, G.; Girerd, J.-J. *J. Am. Chem. Soc.* **1993**, *115*, 5155−5168.
(26) Macedo, A. L.; Moura, I.; Moura, J. J. G.; LeGall, J.; Huynh, B. H. *Inorg. Chem.* **1993**, *32*, 1101−1105.
(27) (a) Guigliarelli, B.; More, C.; Bertrand, P.; Gayda, J.-P. *J. Chem. Phys.* **1986**, *85*, 2774−2778. (b) Gayda, J.-P.; Bertrand, P.; Theodule, F.-X.; Moura, J. J. G. *J. Chem. Phys.* **1982**, *77*, 3387−3391.
(28) Day, E. P.; Peterson, J.; Bonvoisin, J. J.; Moura, I.; Moura, J. J. G. *J. Biol. Chem.* **1988**, *263*, 3684−3689.
(29) Variable-temperature magnetic susceptibility measurements may provide information about the individual ecc and the degree of bridging asymmetry.